Finite-length EXIT Analysis and Design of Protograph LDPC Codes for Ultra-High-Density Magnetic Recording Channels

Yi Fang, Guojun Han, Yong Liang Guan, Guoan Bi,
Francis C. M. Lau, and Lingjun Kong

Abstract

We study the performance of protograph low-density parity-check (LDPC) codes over two-dimensional (2D) intersymbol interference (ISI) channels in this paper. To begin with, we propose a modified version of finite-length (FL) extrinsic information transfer (EXIT) algorithm so as to facilitate the convergence analysis of protograph codes. Exploiting the FL-EXIT analyses, we observe that the protograph codes optimized for one-dimensional (1D) ISI channels, e.g., the 1D-ISI protograph code, cannot maintain their advantages in the 2D-ISI scenarios. To address this problem, we develop a simple design scheme for constructing a family of rate-compatible improved protograph (RCIP) codes particularly for 2D-ISI channels, which not only outperform the 1D-ISI protograph code, but also are superior to the regular column-weight-3 (CW-3) code and optimized irregular LDPC codes in terms of the convergence speed and error performance. More importantly, such RCIP codes benefit from relatively lower error-floor as well as linear encoding and fast decoding. Thanks to these advantages, the proposed RCIP codes stand out as better alternatives in comparison with other error-correction codes (ECCs) for ultra-high-density data storage systems.

Y. Fang and G. Han are with the School of Information Engineering, Guangdong University of Technology, China. Y. Fang is also with the School of Electrical and Electronic Engineering, Nanyang Technological University, Singapore (email: fangyi@gdut.edu.cn).

Y. L. Guan and G. Bi are with School of Electrical and Electronic Engineering, Nanyang Technological University, Singapore.

F. C. M. Lau is with the Department of Electronic and Information Engineering, Hong Kong Polytechnic University, Hong Kong.

L. Kong is school of Computer Science and Technology, Nanjing University of Posts and Communications, China.

Index Terms

Extrinsic information transfer (EXIT), protograph low-density parity-check (LDPC) codes, turbo equalization, two-dimensional (2D) intersymbol interference (ISI).

I. INTRODUCTION

Intersymbol interference (ISI) is one of the major factors that deteriorate the performance of a variety of communication and magnetic recording systems. The conventional one-dimensional magnetic recording (1DMR) systems are usually modeled as partial response (PR) channels, which can be treated as a rate-1 convolutional encoder. Therefore, the Bahl-Cocke-Jelinek-Raviv (BCJR) detector can provide an optimal error rate over such channels [1]. To improve the error performance further under such channels, precoding or error-correction coding (ECC) have been proposed together with turbo equalization being used at the receiving end [2]–[4]. In the turbo equalization (decoder), the PR channel and ECC are considered as the inner code and outer code as in a turbo code, respectively, such that the constituent detector and decoder at the receiver terminal can exchange their corresponding *extrinsic* soft information iteratively to enhance the system performance. Specifically, a remarkable coding gain can be achieved by utilizing low-density parity-check (LDPC) codes as the ECC [2]. In the past ten years, the design of encoding and decoding schemes for 1DMR systems has been intensely investigated [5], [6]. Today, the industry has been able to approach the date-storage-density limit of 1DMR systems.

Aiming at increasing the data-storage density beyond $1\ \mathrm{Tb/in^2}$, bit-patterned media recording (BPMR), heat-assisted magnetic recording (HAMR), and two-dimensional magnetic recording (2DMR) have been emerged as new promising technologies [7]. As compared with 1DMR systems, the track pitch in the above-mentioned systems has become smaller, which results in severe inter-track interference (ITI). Along with the ISI, these high-density data storage systems suffer from a 2D interference, which significantly degrades the error performance, so that they should be modeled as 2D-ISI channels [8]. Motivated by the superiority of data-storage density, large attention has been turned to 2D-ISI channels. The symmetric information rate (SIR) and the error performance of such channels have been thoroughly analyzed in [9]–[12]. Parallel with the information-theoretical advancements, several sub-optimal detecting algorithms have been developed so as to reduce the complexity of BCJR detector without sacrificing much performance,

e.g., the iterative row-column soft decision feedback algorithm (IRCSDFA) [13] and reduced-state BCJR algorithm [14]. With the employment of Gaussian approximation (GA) approach, the dimension of ISI trellis in a 2D-ISI channel can be reduced, and hence the corresponding channel is simplified to an 1D-ISI channel. In such a framework, the original IRCSDFA combined with a 1D-BCJR algorithm, i.e., GA-IRCSDFA-BCJR algorithm, has been proposed to recover the input data more efficiently [15].

Nevertheless, the error performance of 2DMR systems is not excellent enough to satisfy the requirement of practical applications. In order to overcome this weakness, ECCs and joint iterative decoders (i.e., turbo decoders) have been applied and optimized in 2D-ISI channels [16]–[21]. For example, the binary/non-binary LDPC codes have been designed to achieve SIR-approaching error performance with two different turbo decoders, which involve a symbol-based BCJR (inner) detector [18] and a GA-IRCSDFA-BCJR detector [19], respectively. Furthermore, the turbo decoder has been improved so as to significantly reduce the complexity [20] and enhance the anti-ISI capability [21]. As can be seen, the best-performing irregular LDPC codes in [18], [19], [22] possess too many degree-2 variable nodes (VNs) and thus may suffer from two drawbacks — nonlinear encoding complexity and relatively higher error floor. To deal with the above-mentioned problem, several types of structured LDPC codes that exhibit the linear-minimum-distance property have been proposed. It has been demonstrated that LDPC codes that have minimum distance growing linearly with the codeword length (i.e., linear-minimum-distance property) possess lower error floors as compared to their counterparts that do not show this property [23], [24]. Among all the structured LDPC codes, the protograph (LDPC) codes have attained most attention since they achieve capacity-approaching performance as well as linear encoding and fast decoding [25]. Owing to the aforementioned advantages, protograph codes have been extensively used in a myriad of communication systems, e.g., deep-space communication systems [26], [27], wireless communication systems [28], and data storage systems [5], [29].

To the best of our knowledge, the performance of protograph codes over 2D-ISI channels remains unexplored thus far, there are still substantial problems worth discussing. In this paper, we conduct a comprehensive investigation on the design and analysis of protograph codes in such challenging transmission environments. Firstly, we extend the finite-length (FL) extrinsic information transfer (EXIT) algorithm for accurately analyzing the convergence performance of protograph codes. The results suggest that the optimized protograph codes for 1D-ISI channels

(e.g., the 1D-ISI protograph code) are inferior to the regular column-weight-3 (CW-3) code [31], and hence may not be applicable to 2D-ISI channels directly. To overcome the disadvantage, we further propose a simple design approach so as to construct a family of rate-compatible improved protograph (RCIP) codes with various code rates ranging from $1/2$ to $1-\zeta$ (ζ is an arbitrarily small positive value). The theoretical analyses and simulated results illustrate that the proposed high-rate RCIP codes possess both larger decoding tunnels and better performance as compared to the 1D-ISI protograph code, regular CW-3 code, and optimized irregular LDPC codes, especially in the high signal-to-noise-ratio (SNR) region. Accordingly, the RCIP codes that benefit from the low complexity, excellent performance, and linear-minimum-distance property appear to be very good candidates for use in ultra-high-density magnetic recoding systems.

The rest of this paper is organized as follows. In Section II, we introduce the system model and basic principles. The modified FL-EXIT algorithm and decoding tunnel are elaborated in Section III, while the detailed analyses and design of protograph codes are carried out in Section IV. In Sections V and VI, we present the simulation results and give the concluding remarks, respectively.

II. System Model

In 2DMR systems, each bit suffers from not only the ISI in the down-track direction but also the ITI in the cross-track direction. Therefore, the channel-impulse-response (CIR) matrix can be expressed by

$$\mathcal{H} = \begin{pmatrix} h_{1,1} & h_{1,2} & \cdots & h_{1,\kappa_t} \\ h_{2,1} & h_{2,2} & \cdots & h_{2,\kappa_t} \\ \vdots & \vdots & \ddots & \vdots \\ h_{\kappa_s,1} & h_{\kappa_s,2} & \cdots & h_{\kappa_s,\kappa_t} \end{pmatrix}, \tag{1}$$

where κ_s and κ_t denote the numbers of magnetic islands that the read head senses in the cross-track and down-track directions, respectively. In practice, the ITI is mainly resulted from the adjacent track on each side of the primary track and the ITI from nonadjacent tracks can be ignored [20], which leads to an $\mathcal{H}$ matrix with $\kappa_s = 3$. In this paper, we focus our attention on the scenario with $\kappa_s = 3$ and $\kappa_t = 3$, which is commonly utilized in a myriad of 2DMR research [15]–[21]. Furthermore, if the read head partially spans the outer tracks, the CIR matrix

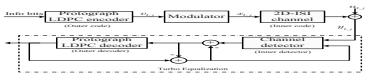

Fig. 1. System model of the protograph codes over a 2D-ISI channel.

is yielded as

$$\mathcal{H} = \begin{pmatrix} \beta & b & \beta \\ \alpha & a & \alpha \\ \beta & b & \beta \end{pmatrix}. \tag{2}$$

Unless otherwise mentioned, we assume that the recording density of the 2DMR system is $4\ \mathrm{Tb/in^2}$ [15], [17], [18], for which the CIR matrix is reduced to

$$\mathcal{H}_{4\mathrm{T}} = \begin{pmatrix} 0.0368 & 0.1435 & 0.0368 \\ 0.2299 & 0.8966 & 0.2299 \\ 0.0368 & 0.1435 & 0.0368 \end{pmatrix}. \tag{3}$$

The system model of the protograph codes over a 2D-ISI channel is illustrated in Fig. 1. Referring to this figure, the information bits (info bits) of length K are firstly encoded exploiting the binary protograph code of length N. Subsequently, the coded bits $v_{l,j} \in \{0, 1\}$ are modulated into $x_{l,j} = (-1)^{v_{l,j}} \in \{+1, -1\}$, which will be distributed in an array of size $L_m \times L_n$. The readback signal corresponding to the j-th modulated bit of the l-th track can be described as

$$y_{l,j} = \sum_{s=1}^{\kappa_s} \sum_{t=1}^{\kappa_t} h_{s,t} x_{l-s,j-t} + n_{l,j}, \tag{4}$$

where $1 \le l \le L_m, 1 \le j \le L_n, N = L_m \times L_n$; $h_{s,t}$ is the element in the s-th row and t-th column of the CIR matrix $\mathcal{H}$ of size $\kappa_s \times \kappa_t$; $n_{l,j} \sim \mathcal{N}(0, \sigma_n^2)$ denotes additive white Gaussian noise (AWGN) with zero mean and variance $\sigma_n^2 = N_0/2$, and N_0 denotes the noise power-spectral density. We assume that $x_{l,j} = -1$ for all $(l, j) \notin \{(l, j) : 1 \le l \le L_m, 1 \le j \le L_n\}$.

At the receiver, a joint iterative decoding scheme (turbo equalization) is exploited to retrieve the original data bits, in which the inner detector is implemented by the symbol-based BCJR

[1] or GA-IRCSDFA-BCJR algorithms [15] while the outer decoder is performed by the belief propagation algorithm (BP) [32], [33]. *Note that* we do not consider the written-in error and the interleaver in our system. The SNR per information bit, i.e., E_b/N_0, is defined as

$$\frac{E_b}{N_0} = \frac{(E_s/N_0)}{R} = \frac{\sum_{s=1}^{\kappa_s}\sum_{t=1}^{\kappa_t}(h_{s,t})^2}{2R\sigma_n^2}, \tag{5}$$

where E_s/N_0 is the SNR per symbol.

III. Modified FL-EXIT Algorithm for Protograph Codes

A. Background and Validation

EXIT chart[1] can be used to evaluate the asymptotic convergence behavior of iterative decoders via tracing the extrinsic mutual information (MI) [32]–[35]. As an asymptotically analytical method, EXIT chart offers an effective way to predict the convergence and error performance of sufficiently long codewords. Unfortunately, for the scenarios of short/moderate codeword length, this analytical tool can no longer work so well because the typicality and ergodicity properties do not hold [36]–[38]. In order to overcome the drawback of EXIT chart, FL analyses have been introduced [5], [36]–[39]. In particular, two novel FL-EXIT algorithms have been proposed to determine the convergence performance of protograph codes in PR channels [5] and the protograph-based joint channel-and-physical-layer-network coding schemes in ergodic fading channels [38], respectively.

Distinguished from the IL-EXIT analysis, its FL counterpart admits that the channel ergodicity and the concentration rule may not retain for short or moderate codeword length [37]. Instead of a single EXIT curve, the FL-EXIT algorithm exploits a set of EXIT curves (called as *EXIT band*) to characterize a component code, all of which are attained through Monte Carlo simulation on FL codewords. As a result, the FL-EXIT chart is considered as a more accurate analysis tool for short/moderate codeword length with respect to the IL ones.

Recently, two modified EXIT algorithms have been developed to optimize coded and uncoded 2D-ISI channels, respectively [18], [40]. Nevertheless, the algorithm in [18] is not suitable for protograph codes due to the following reasons.

[1]"EXIT chart" will be used instead of "infinite-length (IL) EXIT chart" in the remainder of this paper for simplicity.

1) Degree-1 VNs and punctured VNs may exist in the protograph codes. However, the EXIT algorithm in [18] is described based on the degree-distribution pair of LDPC codes, in which degree-1 VNs are not allowed and punctured VNs cannot be identified.
2) Some protograph codes that share the same degree-distribution pair may have different protograph structures. For such a scenario, these protograph codes exhibit different convergence behaviors. Yet, the conventional EXIT algorithm [18] cannot distinguish the difference among the aforementioned codes.
3) For finite-length codewords, the conventional EXIT algorithm can not characterize the corresponding convergence performance accurately.

Consequently, we propose a modified version of FL-EXIT algorithm for protograph codes based on [37], which takes into consideration the different edge-connection properties. To facilitate the description of the algorithm, we firstly define some new notations.

- $L_{\mathrm{A,IO/OI}}(l,j)$ $(L_{\mathrm{E,IO/OI}}(l,j))$ denotes the input *a-priori* (output *extrinsic*) log-likelihood-ratio (LLR) of the coded bit $v_{l,j}$ flowing from the inner detector to outer decoder/flowing from the outer detector to inner decoder.
- $I_{\mathrm{A,IO/OI}}$ $(I_{\mathrm{E,IO/OI}})$ denotes the average *a-priori (extrinsic)* MI between the coded bit $v_{l,j}$ and its corresponding input *a-priori* (output *extrinsic*) LLR $L_{\mathrm{A,IO/OI}}(l,j)$ $(L_{\mathrm{E,IO/OI}}(l,j))$.

In the concatenated system, the 2D-ISI channel is treated as the inner code, which is not a binary linear code. More precisely, it has binary-input and real-valued output. For this reason, one should first justify the validity of the FL-EXIT algorithm in this memory channel prior to using it. Specifically, the precondition of the usage of such an algorithm is that the *extrinsic* LLRs output from each soft-input soft-output (SISO) detector/decoder approximately follow a symmetric Gaussian (SG) distribution. As a validation of this precondition, we compare the actual probability density functions (PDFs) of LLRs output from a BCJR detector (i.e., $f(L_{\mathrm{E,IO}}(l,j))$) and the standard SG distribution $\mathcal{N}(\mu_\tau, 2\mu_\tau)$, where $\mu_\tau = \mathbb{E}[L_{\mathrm{E,IO}}(l,j)|v_{l,j}=\tau],\ \text{and}\ \tau \in \{0,1\}$. Assuming the 1D-ISI protograph code [29] with a code rate $R = 7/8$ and length $N = 4800$, Fig. 2 presents the corresponding PDFs of $L_{\mathrm{E,IO}}(l,j)$ and $\mathcal{N}(\mu_\tau, 2\mu_\tau)$ over a 2D-ISI channel with $E_b/N_0 = 4.4$ dB. It indicates that the PDF of $L_{\mathrm{E,IO}}(l,j)$ is approximately consistent with that of $\mathcal{N}(\mu_\tau, 2\mu_\tau)$ for a fixed τ. Simulations have also been performed on other CIR matrices, protograph codes, SNRs, and similar observations are obtained. Hence, the FL-EXIT algorithm

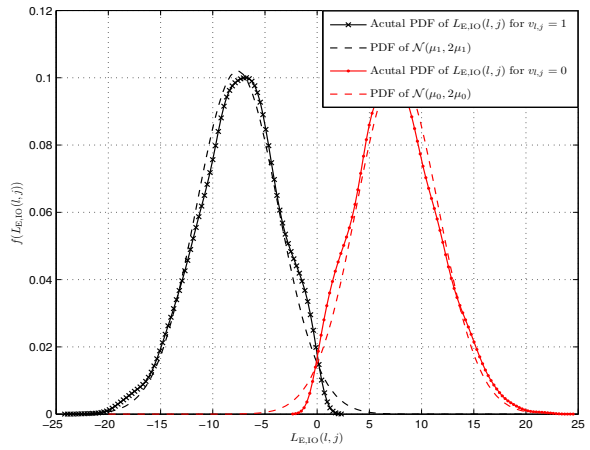

Fig. 2. PDFs of $L_{\mathrm{E,IO}}(l,j)$ and $\mathcal{N}(\mu_\tau, 2\mu_\tau)$ corresponding to the 1D-ISI protograph code over a 2D-ISI channel. The parameters used are $R = 7/8$, $N = 4800$, and $E_b/N_0 = 4.4$ dB.

can be used for analyzing our system.

Remark: In this paper, we measure the consistency between the actual PDF of $L_{\mathrm{E,IO}}(l,j)$ and symmetric Gaussian distribution $\mathcal{N}(\mu_\tau, 2\mu_\tau)$ by comparing their corresponding shapes, as in [5], [37].

B. Modified FL-EXIT Algorithm

Based on the SG assumption, the standard deviation of the (input) *a-priori* LLR sequence $\{L_{\mathrm{A},\Theta}(l,j)\}$ of a detector/decoder can be calculated as [33]

$$\sigma_{\mathrm{A},\Theta} \approx \begin{cases} \eta_1 I_{\mathrm{A},\Theta}^2 + \eta_2 I_{\mathrm{A},\Theta} + \eta_3\sqrt{I_{\mathrm{A},\Theta}}, & \text{if } 0 \le I_{\mathrm{A},\Theta} \le 0.3646, \\ \eta_4 \ln[\eta_5(1 - I_{\mathrm{A},\Theta})] + \eta_6 I_{\mathrm{A},\Theta}, & \text{otherwise}, \end{cases} \tag{6}$$

where $\Theta \in \{\mathrm{IO}, \mathrm{OI}\}$, $I_{\mathrm{A},\Theta}$ is the average MI corresponding to $\{L_{\mathrm{A},\Theta}(l,j)\}$, $\eta_1 = 1.09542, \eta_2 = 0.214217, \eta_3 = 2.33737$, $\eta_4 = -0.706692, \eta_5 = 0.386013$, and $\eta_6 = 1.75017$.

Afterwards, we can evaluate the *a-priori* LLR of a detector/decoder corresponding to $v_{l,j}$ as

$$L_{\mathrm{A},\Theta}(l,j) = (\sigma_{\mathrm{A},\Theta}^2/2)x_{l,j} + n_{\mathrm{L},l,j}, \tag{7}$$

where $n_{\mathrm{L},l,j} \sim \mathcal{N}(0, \sigma_{\mathrm{A},\Theta}^2)$ is the Gaussian-distributed random variable.

Without loss of generality, we define the average *extrinsic* MI output from the inner detector/outer decoder utilizing the actual PDF of the corresponding LLR sequence, as

$$I_{\mathrm{E},\Theta} = \frac{1}{2} \sum_{\tau=\{+1,-1\}} \int_{-\infty}^{\infty} f_{\mathrm{E},\Theta}(\xi|X=\tau) \times \log_2 \frac{2 f_{\mathrm{E},\Theta}(\xi|X=\tau)}{f_{\mathrm{E},\Theta}(\xi|X=+1) + f_{\mathrm{E},\Theta}(\xi|X=-1)} \, \mathrm{d}\xi, \tag{8}$$

where $f_{\mathrm{E},\Theta}(\xi|X=\tau)$ is the conditional PDF of LLR sequence $\{L_{\mathrm{E},\Theta}(l,j)\}$ given $X=(-1)^{v_{l,j}}=\tau\in\{+1,-1\}$.

Based on the aforementioned knowledge, for a fixed E_b/N_0, we can plot the EXIT bands output from the inner detector and outer decoder, respectively, by means of calculating their corresponding *extrinsic* MIs. Each EXIT band is composed of an expected EXIT curve, an upper-bound curve, and a lower-bound curve. The detailed steps of the modified FL-EXIT algorithm are described as follows.

• **Calculating the *extrinsic* MI output from the inner detector**

1) Randomly generate a sequence of information bits $\{s_j\}$ and encode them by a protograph code of length N, denoted as $\{v_{l,j}\}$ $(1\le l\le L_m, 1\le j\le L_n, N=L_m\times L_n)$. The BPSK-modulated sequence $\{x_{l,j}\}$ is readily formed using $x_{l,j}=(-1)^{v_{l,j}}$. Next, for $l=1,2,\cdots,L_m$ and $j=1,2,\cdots,L_n$, the channel initial LLR sequence $\{L_{\mathrm{ch}}(l,j)\}$ is computed by exploiting the received signals of the 2D-ISI channel.
2) For a given *a-priori* MI $I_{\mathrm{A,IO}}\in[0,1]$, the standard derivation $\sigma_{\mathrm{A,IO}}$ of the *a-priori* LLRs is easily obtained utilizing (6). With the help of $\sigma_{\mathrm{A,IO}}$, one can further generate a Gaussian-distributed LLR sequence $\{L_{\mathrm{A,IO}}(l,j)\}$ of length N exploiting (7).
3) The sequences $\{L_{\mathrm{ch}}(l,j)\}$ and $\{L_{\mathrm{A,IO}}(l,j)\}$ are passed through the inner detector to yield the corresponding *extrinsic* LLR sequence $\{L_{\mathrm{E,IO}}(l,j)\}$ of length N. In particular, the relationship among these three variables can be formulated as

$$L_{\mathrm{E,IO}}(l,j)=\mathcal{T}_{\mathrm{inner}}(L_{\mathrm{ch}}(l,j),L_{\mathrm{A,IO}}(l,j)), \tag{9}$$

where $\mathcal{T}_{\mathrm{inner}}(\cdot)$ is used to describe the behavior of LLR-message processor of the inner detector.
4) Based on $\{L_{\mathrm{E,IO}}(l,j)\}$, the conditional PDF $f_{\mathrm{E,IO}}(\xi|X=\tau)$ can be estimated via Monte Carlo histogram, where $\tau\in\{+1,-1\}$. Afterwards, the average *extrinsic* MI $I_{\mathrm{E,IO}}$ corresponding to $\{L_{\mathrm{E,IO}}(l,j)\}$ is measured using (8).
5) Repeat Steps 1) $\sim$ 4) so as to obtain a sufficient set of $I_{\mathrm{E,IO}}$ values. We denote the resultant MI set as $\mathbf{I}_{\mathrm{E,IO}}=(I_{\mathrm{E,IO}}^{(1)},I_{\mathrm{E,IO}}^{(2)},\cdots,I_{\mathrm{E,IO}}^{(Q)})$, where Q is defined as the cardinality of $\mathbf{I}_{\mathrm{E,IO}}$. Subsequently, the mean and variance of $I_{\mathrm{E,IO}}$, i.e., $\mathbb{E}[I_{\mathrm{E,IO}}]$ and $\mathrm{var}[I_{\mathrm{E,IO}}]$, can be readily calculated. Especially, $\mathbb{E}[I_{\mathrm{E,IO}}]$ is considered as the typical MI value for all the FL codewords.
6) Execute Steps 1) $\sim$ 5) for different values of $I_{\mathrm{A,IO}}\in[0,1]$ to get the EXIT band of the inner

detector, which consists of three EXIT curves — an expected EXIT curve $(I_{\mathrm{A,IO}}, \mathbb{E}[I_{\mathrm{E,IO}}])$, an upper-bound curve $(I_{\mathrm{A,IO}}, \mathbb{E}[I_{\mathrm{E,IO}}]+3\sqrt{\mathrm{var}[I_{\mathrm{E,IO}}]})$, and a lower-bound curve $(I_{\mathrm{A,IO}}, \mathbb{E}[I_{\mathrm{E,IO}}]-3\sqrt{\mathrm{var}[I_{\mathrm{E,IO}}]})$.

- **Calculating the *extrinsic* MI output from the outer decoder**

Likewise, the outer decoder can be processed similarly so as to obtain the corresponding EXIT band. To be specific, the relationship between the *a-priori* LLR $I_{\mathrm{A,OI}}$ and its corresponding *extrinsic* LLR $I_{\mathrm{E,OI}}$ is represented by

$$L_{\mathrm{E,OI}}(l,j) = \mathcal{T}_{\mathrm{outer}}(L_{\mathrm{A,OI}}(l,j)), \tag{10}$$

where $\mathcal{T}_{\mathrm{outer}}(\cdot)$ is used to describe the behavior of LLR-message processor of the outer decoder.

As described in Sect. II, the outer decoder is implemented by the BP algorithm, whose performance is determined by the structure of protograph (i.e., base matrix)[2] [27]. Thereby, the value of $L_{\mathrm{E,OI}}(l,j)$ varies for different protographs codes, which leads to different PDFs $f_{\mathrm{E,OI}}(\xi|X=\tau)$.

Based on the sequence $\{L_{\mathrm{E,OI}}(l,j)\}$, the mean and variance of the *extrinsic* MI, i.e., $\mathbb{E}[I_{\mathrm{E,OI}}]$ and $\mathrm{var}[I_{\mathrm{E,OI}}]$, are measured by performing similar operations as the aforementioned Steps 4) and 5).

Finally, one can readily obtain the EXIT band of the outer decoder, in which the constituent expected EXIT curve, upper-bound curve, and lower-bound curve are respectively denoted as $(I_{\mathrm{A,OI}}, \mathbb{E}[I_{\mathrm{E,OI}}])$, $(I_{\mathrm{A,OI}}, \mathbb{E}[I_{\mathrm{E,OI}}]+3\sqrt{\mathrm{var}[I_{\mathrm{E,OI}}]})$, and $(I_{\mathrm{A,OI}}, \mathbb{E}[I_{\mathrm{E,OI}}]-3\sqrt{\mathrm{var}[I_{\mathrm{E,OI}}]})$.

Remarks:

- To ensure the accuracy of the FL-EXIT algorithm, Q should be set to a sufficiently large positive integer. In this paper, we assume that $Q = 5\times 10^4$.
- The EXIT band of the inner detector is dependent on the E_b/N_0 and the CIR matrix $\mathcal{H}$, but is independent of the type of code;
- The EXIT band of the outer decoder is only determined by the type of code.
- As compared with the density-evolution-based algorithm [18], [27], the EXIT-based methods reduce much computation complexity in analyzing the convergence performance without sacrificing the accuracy.

[2]For a given protograph, the types of VNs are specified only by its corresponding base matrix.

- The modified FL-EXIT algorithm can be applicable to not only protograph codes but also other types of ECCs, e.g., conventional LDPC codes [16], [17].

C. Decoding Tunnel

Utilizing the modified FL-EXIT chart, one can easily identify whether the joint decoder converges successfully or not, and compare the convergence speeds among different ECCs. In detail, the joint decoder can converge successfully with an arbitrarily high probability if the two EXIT bands do not have any overlapping region until their *extrinsic* MIs reach one. Moreover, for a codeword that converges successfully, we define the *decoding tunnel* as the region between the expected EXIT curve of the inner detector and that of the outer decoder, expressed as

$$\mathcal{D} = \left\{ (I_{\mathrm{E,OI}}, I_{\mathrm{E,IO}}) : 0 \leq I_{\mathrm{E,OI}} \leq 1, \mathbb{E}^{-1}[I_{\mathrm{E,OI}}] \leq I_{\mathrm{E,IO}} \leq \mathbb{E}[I_{\mathrm{E,IO}}] \right\}, \tag{11}$$

where $I_{\mathrm{A,OI}} = \mathbb{E}^{-1}[I_{\mathrm{E,OI}}] = \Gamma^{-1}(I_{\mathrm{E,OI}})$ is the inverse function of $\mathbb{E}[I_{\mathrm{E,OI}}] = \Gamma(I_{\mathrm{A,OI}})$, and $\Gamma(\cdot)$ is used to describe the behavior of MI processor of the outer decoder. Given fixed E_b/N_0, R, and N, the protograph code having a larger decoding tunnel should accomplish relatively faster convergence speed and better error performance [5], [37], [38].

IV. Analysis and Design of Protograph Codes

A protograph is a Tanner graph with a relatively small number of nodes [25]. A protograph $\mathcal{G} = (\mathcal{V}, \mathcal{C}, \mathcal{E})$ comprises of three sets $\mathcal{V}$, $\mathcal{C}$, and $\mathcal{E}$, which correspond to N_{P} VNs, M_{P} check nodes (CNs), and the associated edges, respectively. Each edge $e_{i,j} \in \mathcal{E}$ connects a VN $v_j \in \mathcal{V}$ to a CN $c_i \in \mathcal{C}$. Unlike conventional Tanner graph, parallel edges are allowed in a protograph. The protograph can also be represented by an $M_{\mathrm{P}} \times N_{\mathrm{P}}$ base matrix $\mathcal{B} = (b_{i,j})$, where $b_{i,j}$ denotes the number of edges connecting v_j to c_i. The derived graph of size $M \times N$, which corresponds to a rate-R protograph code, can be obtained by performing Q times of "copy-and-permute" operations on a protograph, where $M = QM_{\mathrm{P}}, N = QN_{\mathrm{P}}$, and $R = (N - M)/N$. In this paper, we mainly restrict ourselves to the unpunctured protograph codes as in [28]–[30]. Aiming at matching with the high-code-rate requirement for magnetic recoding systems, we assume two different scenarios: 1) $R = 7/8$; $N = 4800$, $E_b/N_0 = 4.4$ dB; and 2) $R = 8/9$, $N = 4860$,

$E_b/N_0 = 4.6$ dB[3]. *Note that* the maximum number of BP iterations for both scenarios is set to $T_{\mathrm{BP,max}} = 30$.

A. Analysis of Existing Protograph Codes

To begin with, we investigate the convergence performance of the 1D-ISI protograph code over 2D-ISI channels. The base matrix of a rate-$1/2$ 1D-ISI protograph code is written as [29]

$$\mathcal{B} = \begin{pmatrix} 1 & 0 & 0 & 1 & 0 & 4 \\ 0 & 1 & 2 & 1 & 2 & 2 \\ 1 & 0 & 0 & 2 & 1 & 1 \end{pmatrix}. \tag{12}$$

The high-rate 1D-ISI protograph can be constructed by adding more columns (i.e., VNs) into the base matrix (12). For instance, the rate-$7/8$ 1D-ISI protograph is obtained by using computer search, whose base matrix is given as

$$\mathcal{B}_{\mathrm{1D}} = \left(\begin{array}{c:cccccccccccccccc} \mathcal{B} & 2 & 0 & 0 & 0 & 0 & 2 & 2 & 0 & 0 & 0 & 0 & 1 & 0 & 0 & 0 & 2 & 0 & 0 \\ & 1 & 2 & 2 & 2 & 1 & 2 & 2 & 2 & 2 & 2 & 2 & 1 & 2 & 2 & 2 & 1 & 2 & 1 \\ & 2 & 1 & 1 & 1 & 2 & 1 & 1 & 1 & 1 & 1 & 1 & 2 & 2 & 1 & 1 & 2 & 1 & 2 \end{array}\right). \tag{13}$$

Since the design in [29] has only considered the 1D interference rather than the 2D interference (i.e., ISI and ITI), the 1D-ISI protograph code may lose its advantages (e.g., good convergence and error performance) in the 2D-ISI scenarios.

For measuring the performance of 1D-ISI protograph code, the regular CW-3 LDPC code [31], which has shown desirable error performance over 2D-ISI channels [15], [17], is considered as a benchmark. Fig. 3 plots the EXIT bands of these two codes with a code rate $R = 7/8$ (scenario 1) in a 2D-ISI channel. As can been seen, the 1D-ISI protograph code, which converges very fast in the 1D-ISI channels, possesses a relatively narrower decoding tunnel as compared to the regular CW-3 code. In other words, it is expected to be inferior to the regular CW-3 LDPC code in terms of convergence and error performance. More importantly, the EXIT band of the outer decoder corresponding to the 1D-ISI protograph code slightly overlaps with that of the inner detector when $I_{\mathrm{A,IO}} \in [0.9, 1.0]$. Besides, we have tested the punctured improved accumulate-repeat-accumulate (IARA) codes in [5] over 2D-ISI channels and have also observed these codes

[3]A higher SNR $E_b/N_0 = 4.6$ dB is assumed in scenario 2 since most LDPC codes with a code rate $R = 8/9$ may not perform well when $E_b/N_0 = 4.4$ dB.

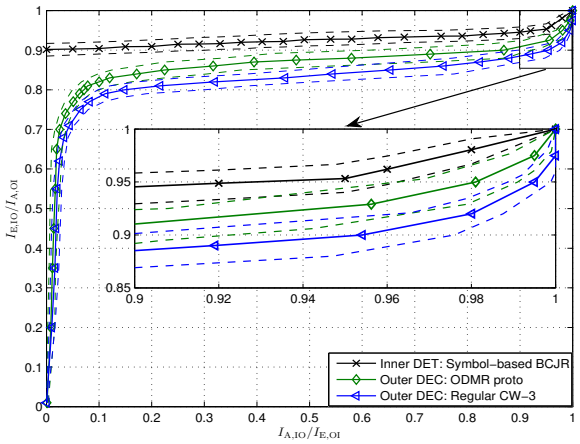

Fig. 3. EXIT bands of the 1D-ISI protograph code and regular CW-3 LDPC code with a code rate $R = 7/8$ (scenario 1) in a 2D-ISI channel. The expected EXIT curves are denoted by the solid lines while the upper-bound curves and lower-bound curves are denoted by the dotted lines. A symbol-based BCJR detector is assumed.

converge slower than the regular CW-3 code in the context of 2D-ISI. As a result, the protograph codes designed particularly for 1D-ISI channels may be not suitable for 2D-ISI applications and hence need to be re-designed[4].

B. Design of RCIP codes

In AWGN and 1D-ISI channels, most research effort has been made to design a rate-$1/2$ excellent protograph code initially, such as the accumulate-repeat-3-accumulate (AR3A) code, accumulate-repeat-by-4-jagged-accumulate (AR4JA) code, 1D-ISI protograph code, and afterwards the corresponding designs have been extended for achieving rate-compatibility (i.e., high code-rate) [5], [26], [27], [29]. Likewise, we also adopt such a methodology to conduct the design of RCIP codes here.

Assuming a rate-$1/2$ protograph code corresponding to a 3×6 base matrix, we firstly fix one smallest-degree VN (i.e., degree-2 VN[5]) and one degree-4 VN, and promptly get the initialized

[4]*It should be noted that* this conjecture only holds for the protograph codes designed particularly for 1D-ISI channels.

[5]As we focus our attention on the unpunctured protograph codes in this paper, there is no precoding structure (i.e., degree-1 VN) in the considered codes.

base matrix as

$$\mathcal{B}' = \begin{pmatrix} 1 & 1 & b_{1,3} & b_{1,4} & b_{1,5} & b_{1,6} \\ 1 & 2 & b_{2,3} & b_{2,4} & b_{2,5} & b_{2,6} \\ 0 & 1 & b_{3,3} & b_{3,4} & b_{3,5} & b_{3,6} \end{pmatrix}. \tag{14}$$

Since linear-minimum-distance property of the protograph codes is very sensitive to the proportion of degree-2 VNs [5], [26], one should limit the fraction of degree-2 VNs[6] and impose a constraint on such VNs [5] to ensure this property. Accordingly, we set the maximum number of degree-2 VNs to 2 (i.e., the first and the last VNs) and assume that no loop exists in the sub-graph which includes all the degree-2 VNs as well as the associated CNs and edges. Further, we assume $b_{i,j} \in \{0, 1, 2, 3\}$ so as to maintain the low-complexity property of protograph codes. Based on the aforementioned assumptions, the objective of our optimization problem is converted to resolving the following function under the turbo decoder

$$\max_{\{b_{i,j}\}} \mathcal{D}, \tag{15}$$

which is subject to

$$\begin{cases} b_{i,j} \in \{0, 1, 2, 3\}, \\ \sum_{i=1}^{3} b_{i,j} \geq 3, \quad j = 3, 4, 5, \\ \sum_{i=1}^{3} b_{i,j} \geq 2, \quad j = 6, \\ b_{1,6} + b_{2,6} = 1, \quad \text{if } \sum_{i=1}^{3} b_{i,6} = 2, \\ I_{\mathrm{A,OI}} < \mathbb{E}[I_{\mathrm{E,IO}}], \quad \forall I_{\mathrm{A,OI}} \in [0, 1). \end{cases}$$

After a simple search, the base matrix of the rate-$1/2$ RCIP code, which exhibits both the largest decoding tunnel and the linear-minimum-distance property, becomes

$$\mathcal{B}' = \begin{pmatrix} 1 & 1 & 0 & 2 & 0 & 0 \\ 1 & 2 & 1 & 1 & 3 & 1 \\ 0 & 1 & 2 & 0 & 0 & 1 \end{pmatrix}. \tag{16}$$

Here, the inner detector of the turbo decoder is implemented by the symbol-based BCJR algorithm [1]. Nevertheless, this result can also be applied to the cases of other inner detectors (e.g.,

[6]The fraction of degree-d_ω ($\omega = 1, 2, \cdots$) VNs is defined as the fraction of edges emanating from such VNs as in the degree distribution [33].

the GA-IRCSDFA-BCJR detector [15]) without any modification since the EXIT band of the inner decoder is independent of the type of code.

In order to extend the base matrix to higher code-rate, the existing rate-$1/2$ protograph code is concatenated with a virtual sub-code that possesses the linear-minimum-distance property. More specifically, inspired by the structure of high-rate AR3A codes, we realize the virtual sub-code by connecting $3n$ new degree-3 VNs to the existing CNs that belong to the rate-$1/2$ RCIP code, whose base matrix is expressed as

$$\mathcal{B}_{\mathrm{SC}} = \begin{pmatrix} \overbrace{0 \;\; 1 \;\; 2 \;\; \cdots \;\; 0 \;\; 1 \;\; 2}^{3n \text{ columns}} \\ 1 \;\; 1 \;\; 1 \;\; \cdots \;\; 1 \;\; 1 \;\; 1 \\ 2 \;\; 1 \;\; 0 \;\; \cdots \;\; 2 \;\; 1 \;\; 0 \end{pmatrix} \tag{17}$$

in which the 1-st, 2-nd, and 3-rd columns are repeated in the $3n$ columns. Then, combining (16) with (17) yields the base matrix of the overall RCIP code

$$\mathcal{B}_{\mathrm{RCIP}} = (\mathcal{B}' \,|\, \mathcal{B}_{\mathrm{SC}}) = \left(\begin{array}{c|c} & \overbrace{0 \;\; 1 \;\; 2 \;\; \cdots \;\; 0 \;\; 1 \;\; 2}^{3n \text{ columns}} \\ \mathcal{B}' & 1 \;\; 1 \;\; 1 \;\; \cdots \;\; 1 \;\; 1 \;\; 1 \\ & 2 \;\; 1 \;\; 0 \;\; \cdots \;\; 2 \;\; 1 \;\; 0 \end{array}\right), \tag{18}$$

The structure of the overall RCIP code is shown in Fig. 4, where $c_j \in \mathcal{C}' = \mathcal{C}_{\mathrm{SC}}$ are the shared CNs connecting to both the rate-$1/2$ RCIP code and the virtual sub-code. According to (18) and Fig. 4, the code rate of the overall RCIP code is $R = (3n+3)/(3n+6) = (n+1)/(n+2),$ where $n = 0, 1, \cdots$, and the fraction of degree-2 VNs is readily computed as $\lambda_{\mathrm{RCIP},2} = (2 \times 2)/(2 \times 2 + 3 \times 3 + 4 + 3n \times 3) = 4/(17 + 9n)$. *Note also that* the family of RCIP codes can benefit from the linear-minimum-distance property.

C. Comparison of Convergence Performance

As a validation of our proposed design, we now examine the convergence performance of the RCIP codes in scenarios 1 and 2 by means of IL and FL-EXIT algorithms. To make an insightful analysis, we consider both the symbol-based BCJR algorithm and GA-IRCSDFA-BCJR algorithm as the realizations of inner detector, and test the optimized irregular LDPC codes [18], [19] (denoted as irregular LDPC code A and irregular LDPC code B) corresponding

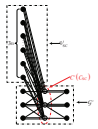

Fig. 4. The protograph $\mathcal{G}_{\mathrm{RCIP}} = (\mathcal{V}' \cup \mathcal{V}_{\mathrm{SC}}, \mathcal{C}', \mathcal{E}' \cup \mathcal{E}_{\mathrm{SC}})$ of the overall RCIP code. $\mathcal{G}' = (\mathcal{V}', \mathcal{C}', \mathcal{E}')$ and $\mathcal{G}_{\mathrm{SC}} = (\mathcal{V}_{\mathrm{SC}}, \mathcal{C}_{\mathrm{SC}}, \mathcal{E}_{\mathrm{SC}})$ denote the prtographs of the rate-$1/2$ RCIP code and the virtual sub-code, respectively.

to these two detecting algorithms, respectively, in scenario 2[7]. The VN-degree distributions of the rate-$8/9$ irregular LDPC code A [18] and irregular LDPC code B [19] are given by

$$\lambda_{\mathrm{A}}(x) = 0.1445x + 0.8146x^2 + 0.0378x^8 + 0.0031x^9, \tag{19a}$$

$$\lambda_{\mathrm{B}}(x) = 0.143x + 0.7824x^2 + 0.0746x^{12}, \tag{19b}$$

while CN-degree distribution of the two irregular LDPC codes is $\rho_{\mathrm{A/B}}(x) = x^{26}$.

1) AWGN Channel: To begin with, the decoding thresholds of the LDPC codes with code rates $R = 7/8$ (scenario 1) and $R = 8/9$ (scenario 2) over an AWGN channel are calculated and listed in Table I and Table II, respectively. As illustrated, the regular CW-3 LDPC code possesses the lowest decoding threshold over both scenarios and hence should exhibit the best convergence performance over AWGN channels.

2) 2D-ISI Channel: Fig. 5 depicts the expected EXIT curves[8] of the proposed RCIP code, 1D-ISI protograph code, and regular CW-3 LDPC code with a code rate $R = 7/8$ (scenario 1) in a 2D-ISI channel. Referring to this figure, the proposed RCIP code provides the largest

[7]The code rate of optimized irregular codes in [18], [19] is $R = 8/9$ so that we are unable to compare the convergence performance between these codes and the proposed RCIP code in scenario 1.

[8]The upper-bound and lower-bound of the EXIT bands in Figs. 5 and 6 are omitted for simplicity.

TABLE I

DECODING THRESHOLDS $(E_b/N_0)_{\text{th}}$ (dB) OF THE PROPOSED RCIP CODE, 1D-ISI PROTOGRAPH CODE, AND REGULAR CW-3 LDPC CODE WITH A CODE RATE $R = 7/8$ (SCENARIO 1) OVER AN AWGN CHANNEL. CHANNEL CAPACITY EQUALS 2.845 dB.

Code Type	1D-ISI proto	Regular CW-3	Proposed RCIP
$(E_b/N_0)_{\text{th}}$	3.388	3.283	3.331

TABLE II

DECODING THRESHOLDS $(E_b/N_0)_{\text{th}}$ (dB) OF THE PROPOSED RCIP CODE, REGULAR CW-3 LDPC CODE, IRREGULAR LDPC CODE A, AND IRREGULAR LDPC CODE B WITH A CODE RATE $R = 8/9$ (SCENARIO 2) OVER AN AWGN CHANNEL. CHANNEL CAPACITY EQUALS 3.042 dB.

Code Type	Regular CW-3	Irregular A	Irregular B	Proposed RCIP
$(E_b/N_0)_{\text{th}}$	3.453	3.557	3.487	3.502

decoding tunnel while the 1D-ISI protograph code produces the smallest one for a fixed detecting algorithm. Consequently, the RCIP code achieves additional gains as compared to the other two codes in terms of convergence and error performance.

Fig. 6 further presents the expected EXIT curves of the proposed RCIP code, regular CW-3 LDPC code, and optimized irregular LDPC codes with a code rate $R = 8/9$ (scenario 2) in a 2D-ISI channel. We can observe that the two irregular LDPC codes, which exhibit similar

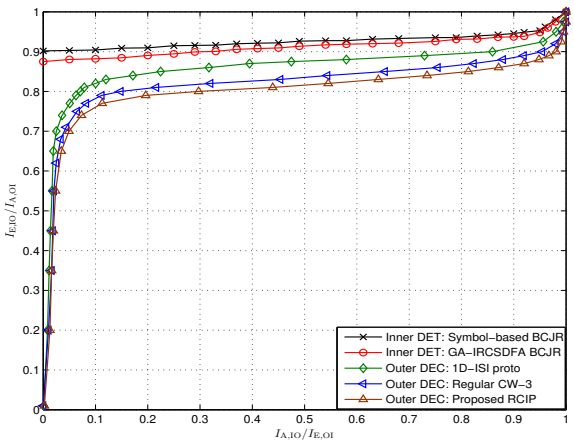

Fig. 5. Expected EXIT curves of the proposed RCIP code, 1D-ISI protograph code, and regular CW-3 LDPC code with a code rate $R = 7/8$ (scenario 1) in a 2D-ISI channel.

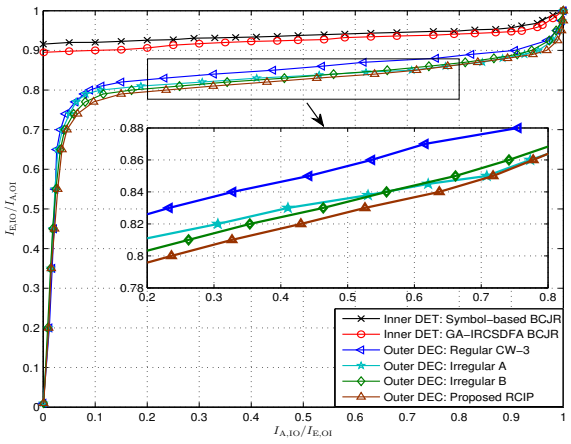

Fig. 6. Expected EXIT curves of the proposed RCIP code, regular CW-3 LDPC code, irregular LDPC code A, and irregular LDPC code B with a code rate $R = 8/9$ (scenario 2) in a 2D-ISI channel.

convergence performance, outperform the regular CW-3 LDPC code. However, the two optimized LDPC codes converge slower than the proposed RCIP code because of a slightly smaller decoding tunnel. Accordingly, the proposed RCIP codes can accomplish superb convergence performance with various high code-rates.

To summarize, the proposed RCIP code, which is outperformed by the regular CW-3 LDPC code and the optimized irregular LDPC code B over AWGN channels, converges faster than these two types of LDPC codes over 2D-ISI channels. As proved in [41], LDPC codes having good performance over AWGN channels can also perform well over other types of memoryless channels. Nonetheless, this conclusion does not hold over channels with memory, such as the magnetic recording channels and non-ergodic block-fading channels [38]. Due to this reason, LDPC codes, including protograph codes, should be re-constructed before applying to transmission environments with memory.

V. Simulation Results

In this section, the simulated bit error rates (BERs) and word error rates (WERs) of the proposed RCIP codes, 1D-ISI protograph code, as well as conventional LDPC codes over 2D-ISI channels are presented. Unless otherwise stated, the CIR matrix is assumed as (3) and the maximum number of turbo iterations is set to $T_{\mathrm{T,max}} = 10$. Similar to Sect. IV, we also consider two different scenarios (scenarios 1 and 2) and two different inner detectors (symbol-based BCJR

detector and GA-IRCSDFA-BCJR detector).

We firstly simulate the BERs and WERs of the proposed RCIP code, 1D-ISI protograph code, and regular CW-3 LDPC code with a code rate $R = 7/8$ (scenario 1) in a 2D-ISI channel and show the results in Fig. 7. As observed from Fig. 7(a) where the inner detector is implemented by the symbol-based BCJR algorithm, the regular CW-3 LDPC code obtains a gain of 0.2 dB over the 1D-ISI protograph code at a BER of 3×10^{-7}, while the proposed RCIP code attains an additional gain of 0.1 dB over the regular CW-3 LDPC code. In the same figure, we also observe that the RCIP code, regular CW-3 LDPC code, and 1D-ISI protograph code respectively achieve BERs of $3 \times 10^{-8}, 2 \times 10^{-7}$, and 4×10^{-6} at $E_b/N_0 = 4.6$ dB. Moreover, at a BER of 10^{-6}, the proposed RCIP code is only 0.75 dB away from SIR[9], which is expected to be reduced as the codeword length increases. In addition, the relative error performance among the codes remains the same for the simplified GA-IRCSDFA-BCJR detector referring to Fig. 7(b). Yet, for a fixed LDPC code, the GA-IRCSDFA-BCJR detector that possesses relatively lower implementation complexity suffers from a performance degradation of about 0.3 dB as compared with the symbol-based BCJR detector.

Fig. 8 compares the simulated BER and WER results of the proposed RCIP code, regular CW-3 code, and optimized irregular LDPC codes with a code rate $R = 8/9$ (scenario 2) in a 2D-ISI channel. As shown in Fig. 8(a), the irregular LDPC code A outperforms the regular CW-3 LDPC code in the low-SNR region ($E_b/N_0 < 4.6$ dB). However, this irregular LDPC code exhibits the error-floor behavior in the high-SNR region ($E_b/N_0 \geq 4.6$ dB) and becomes inferior to the regular CW-3 LDPC code. According to (19a) and (19b), both the irregular code A and irregular code B possess a substantially large fraction of degree-2 VNs (i.e., $\lambda_{\mathrm{A},2} = 14.45\%$ and $\lambda_{\mathrm{A},2} = 14.3\%$), which may result in an error-floor. On the contrary, the proposed RCIP code, which has a small fraction of degree-2 VNs ($\lambda_{\mathrm{RCIP},2} = 5\%$ when $R = 8/9$, i.e., $n = 7$) as well as the linear-minimum-distance property, produces excellent error performance for the range of E_b/N_0 under study and is the best-performing code. For example, at a BER of 10^{-6}, the

[9]As the capacity derivation for 1D/2D-ISI channels is still an open problem nowadays, the SIR is used to provide the fundamental lower-limit on the achievable rate to realize reliable communication in such channels instead [9], [10]. In this paper, the SIRs are calculated in a similar way as those in [10], [18]. However, we omit the calculation procedure of SIR here but refer the interested readers to the aforementioned literature as well as the references therein for more details since it is outside the scope of this paper.

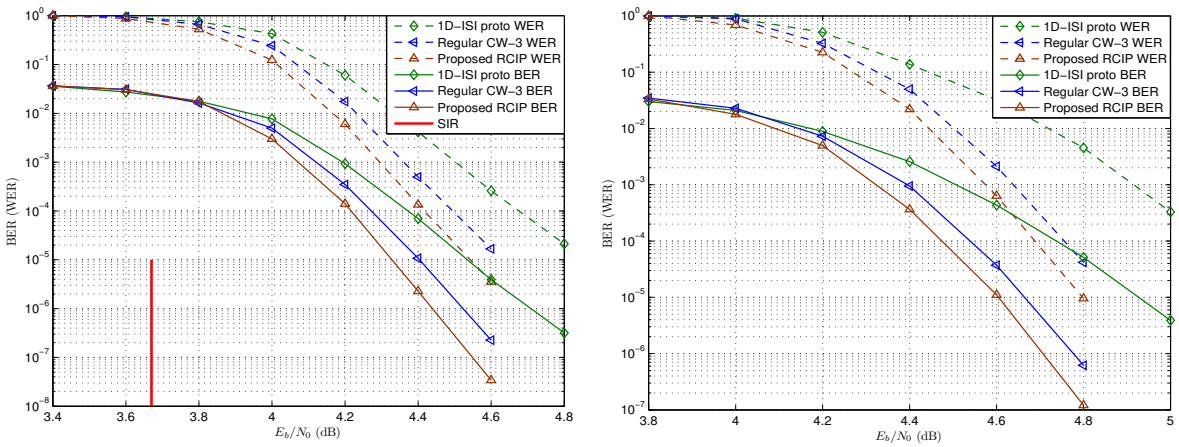

(a) (b)

Fig. 7. Simulated BER and WER curves of the proposed RCIP code, 1D-ISI protograph code, and regular CW-3 LDPC code with a code rate $R = 7/8$ (scenario 1) in a 2D-ISI channel. The inner detectors are implemented by the (a) symbol-based BCJR algorithm and (b) GA-IRCSDFA-BCJR algorithm, respectively.

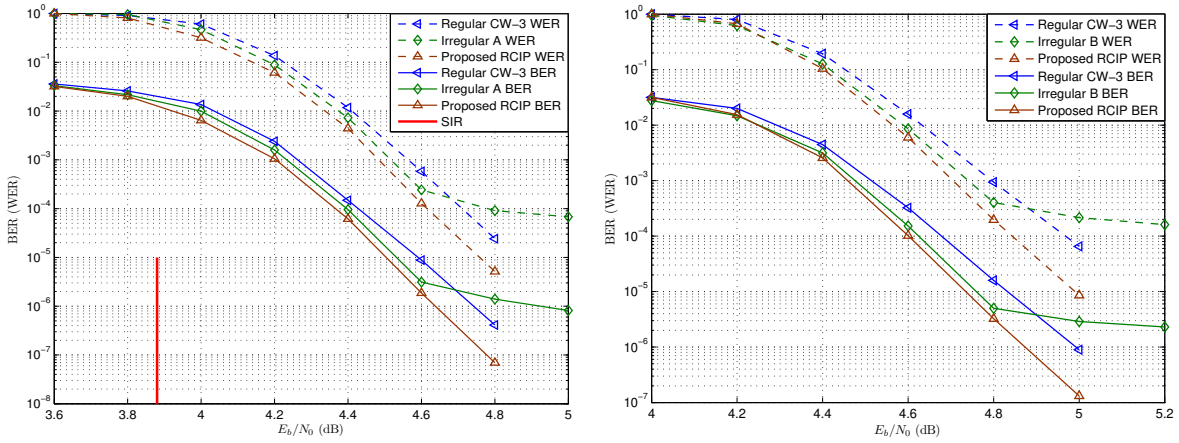

(a) (b)

Fig. 8. Simulated BER and WER curves of the proposed RCIP code, regular CW-3 LDPC code, and optimized irregular LDPC codes with a code rate $R = 8/9$ (scenario 2) in a 2D-ISI channel. The inner detectors are implemented by the (a) symbol-based BCJR algorithm and (b) GA-IRCSDFA-BCJR algorithm, respectively.

rate-$8/9$ RCIP code possesses a gap of 0.75 dB to the corresponding SIR. Similar observations are also made from the results for the GA-IRCSDFA-BCJR detector in Fig. 8(b). *Note that* the relative performance among the codes in WER is reasonably consistent with that in BER for both scenarios.

Furthermore, we have performed the simulations for the proposed RCIP code, 1D-ISI pro-

tograph code, regular CW-3 LDPC codes, and optimized irregular LDPC codes in the 2D-ISI channels with other CIR matrices, such as $\mathcal{H}$ matrices in [20], and have obtained similar results. In summary, the LDPC codes, from the best to the worst convergence and error performance in 2D-ISI channels, are ranked in the following order: 1) RCIP code, 2) optimized irregular LDPC codes, 3) regular CW-3 LDPC code, and 4) 1D-ISI protograph code.

VI. Conclusions

In this work, the performance of protograph codes over 2D-ISI channels has been carefully studied. Utilizing a modified FL-EXIT chart, the decoding tunnel has been derived to characterize the convergence performance of protograph codes. Based on the proposed analytical tools, we have found that the existing protograph codes do not show any superiority in such transmission scenarios. Aiming at dealing with this problem, we have further developed a systematic procedure so as to search for a superior family of protograph codes, namely RCIP codes, which enable large decoding tunnels as well as the linear-minimum-distance property. The convergence analyses and BER simulations have both indicated that the proposed RCIP codes not only outperform the 1D-ISI protograph code, regular CW-3 LDPC code, and optimized irregular LDPC codes with a wide range of code rates lower-bounded by $1/2$, but also achieve desirable gaps to the corresponding SIRs. In particular, the RCIP codes possess some very attractive superiorities, such as lower error floor and low complexity, which are very promising for the ultra-high-density magnetic recording applications.

References

[1] L. Bahl, J. Cocke, F. Jelinek, and J. Raviv, "Optimal decoding of linear codes for minimizing symbol error rate," *IEEE Trans. Inf. Theory*, vol. 20, no. 2, pp. 284–287, Mar. 1974.

[2] H. Song, R. Todd, and J. Cruz, "Low density parity check codes for magnetic recording channels," *IEEE Trans. Magn.*, vol. 36, no. 5, pp. 2183–2186, Sept. 2000.

[3] K. Narayanan, "Effect of precoding on the convergence of turbo equalization for partial response channels," *IEEE J. Sel. Areas Commun.*, vol. 19, no. 4, pp. 686–698, Apr. 2001.

[4] C. Douillard, M. Jezequel, C. Berrou, A. Picart, P. Didier, and A. Glavieux, "Iterative correction of intersymbol interference: Turbo-equalization," *European Trans. on Telecommun.*, vol. 6, no. 5, pp. 507–511, Sept. 1995.

[5] Y. Fang, P. Chen, L. Wang, and F. C. M. Lau, "Design of protograph LDPC codes for partial response channels," *IEEE Trans. Commun.*, vol. 60, no. 10, pp. 2809–2819, Oct. 2012.

[6] Y. Han and W. Ryan, "Low-floor detection/decoding of LDPC-coded partial response channels," *IEEE J. Sel. Areas Commun.*, vol. 28, no. 2, pp. 252–260, Feb. 2010.

[7] S. Karakulak, P. Siegel, J. Wolf, and H. Bertram, "A new read channel model for patterned media storage," *IEEE Trans. Magn.*, vol. 44, no. 1, pp. 193–197, Jan. 2008.

[8] Y. Ng, K. Cai, B. Kumar, S. Zhang, and T. C. Chong, "Modeling and two-dimensional equalization for bit-patterned media channels with media noise," *IEEE Trans. Magn.*, vol. 45, no. 10, pp. 3535–3538, Oct. 2009.

[9] J. Chen and P. Siegel, "On the symmetric information rate of two-dimensional finite-state ISI channels," *IEEE Trans. Inf. Theory*, vol. 52, no. 1, pp. 227–236, Jan. 2006.

[10] O. Shental, N. Shental, S. Shamai (Shitz), I. Kanter, A. J. Weiss, and Y. Weiss, "Discrete-input two-dimensional Gaussian channels with memory: Estimation and information rates via graphical models and statistical mechanics," *IEEE Trans. Inf. Theory*, vol. 54, no. 4, pp. 1500–1513, Apr. 2008.

[11] S. Nabavi, S. Jeon, and B. Kumar, "An analytical approach for performance evaluation of bit-patterned media channels," *IEEE J. Sel. Areas Commun.*, vol. 28, no. 2, pp. 135–142, Feb. 2010.

[12] A. Kavcic, X. Huang, B. Vasic, W. Ryan, and M. Erden, "Channel modeling and capacity bounds for two-dimensional magnetic recording," *IEEE Trans. Magn.*, vol. 46, no. 3, pp. 812–818, Mar. 2010.

[13] T. Cheng, B. Belzer, and K. Sivakumar, "Row-column soft-decision feedback algorithm for two-dimensional intersymbol interference," *IEEE Signal Process. Letters*, vol. 14, no. 7, pp. 433–436, Jul. 2007.

[14] J. Yao, K. C. Teh, and K. H. Li, "Reduced-state Bahl-Cocke-Jalinek-Raviv detector for patterned media storage," *IEEE Trans. Magn.*, vol. 46, no. 12, pp. 4108–4110, Dec. 2010.

[15] J. Zheng, X. Ma, Y. L. Guan, K. Cai, and K. S. Chan, "Low-complexity iterative row-column soft decision feedback algorithm for 2-D inter-symbol interference channel detection with Gaussian approximation," *IEEE Trans. Magn.*, vol. 49, no. 8, pp. 4768–4773, Aug. 2013.

[16] X. Liu, C. Shi, M. Teng, and X. Ma, "Error correction coding with LDPC codes for patterned media storage," *IEEE Trans. Magn.*, vol. 45, no. 10, pp. 3745–3748, Oct. 2009.

[17] K. Cai, Z. Qin, S. Zhang, Y. Ng, K. Chai, and R. Radhakrishnan, "Modeling, detection, and LDPC codes for bit-patterned media recording," in *Proc. IEEE GLOBECOM Workshops (GC Wkshps)*, Dec. 2010, pp. 1910–1914.

[18] L. Kong, Y. Guan, J. Zheng, G. Han, K. Cai, and K.-S. Chan, "EXIT-chart-based LDPC code design for 2D ISI channels," *IEEE Trans. Magn.*, vol. 49, no. 6, pp. 2823–2826, Jun. 2013.

[19] Y. L. Guan, G. Han, L. Kong, K. S. Chan, K. Cai, and J. Zheng, "Coding and signal processing for ultra-high density magnetic recording channels," in *Proc. Int. Conf. Comput., Netw. and Commun. (ICNC)*, Feb. 2014, pp. 194–199.

[20] J. Yao, K. C. Teh, and K. H. Li, "Joint iterative detection/decoding scheme for discrete two-dimensional interference channels," *IEEE Trans. Commun.*, vol. 60, no. 12, pp. 3548–3555, Dec. 2012.

[21] G. Han, Y. L. Guan, K. Cai, and K. S. Chan, "Asymmetric iterative multi-track detection for 2-D non-binary LDPC-coded magnetic recording," *IEEE Trans. Magn.*, vol. 49, no. 10, pp. 5215–5221, Oct. 2013.

[22] G. Han, Y. L. Guan, L. Kong, K. S. Chan, and K. Cai, "Towards optimal edge weight distribution and construction of field-compatible low-density parity-check codes over GF(q)," *IET Commun.*, vol. 8, no. 18, pp. 3215–3222, Jul. 2014.

[23] S. Litsyn and V. Shevelev, "On ensembles of low-density parity-check codes: asymptotic distance distributions," *IEEE Trans. Inf. Theory*, vol. 48, no. 4, pp. 887–908, Apr. 2002.

[24] Y. Fang, P. Chen, L. Wang, F. C. M. Lau, and K.-K. Wong, "Performance analysis of protograph-based low-density parity-check codes with spatial diversity," *IET Commun.*, vol. 6, no. 17, pp. 2941–2948, Nov. 2012.

[25] J. Thorpe, "Low-density parity-check (LDPC) codes constructed from protographs," in *Proc. IPN Progress Report*, Aug. 2003, pp. 1–7.

[26] A. Abbasfar, D. Divsalar, and K. Yao, "Accumulate-repeat-accumulate codes," *IEEE Trans. Commun.*, vol. 55, no. 4, pp. 692–702, Apr. 2007.

[27] D. Divsalar, S. Dolinar, C. Jones, and K. Andrews, "Capacity-approaching protograph codes," *IEEE J. Sel. Areas Commun.*, vol. 27, no. 6, pp. 876–888, Aug. 2009.

[28] Y. Fang, G. Bi, and Y. L. Guan, "Design and analysis of root-protograph LDPC codes for non-ergodic block-fading channels," *IEEE Trans. Wireless Commun.*, vol. 14, no. 2, pp. 738–749, Feb. 2015.

[29] T. V. Nguyen, A. Nosratinia, and D. Divsalar, "Rate-compatible protograph-based LDPC codes for inter-symbol interference channels," *IEEE Commun. Lett.*, vol. 17, no. 8, pp. 1632–1635, Aug. 2013.

[30] H. Uchikawa, "Design of non-precoded protograph-based LDPC codes," in *Proc. IEEE Int. Symp. Inf. Theory (ISIT)*, Jun. 2014, pp. 2779–2783.

[31] J. Li, K. Narayanan, E. Kurtas, and C. Georghiades, "On the performance of high-rate TPC/SPC codes and LDPC codes over partial response channels," *IEEE Trans. Commun.*, vol. 50, no. 5, pp. 723–734, May 2002.

[32] S. ten Brink, "Convergence behavior of iteratively decoded parallel concatenated codes," *IEEE Trans. Commun.*, vol. 49, no. 10, pp. 1727–1737, Oct. 2001.

[33] S. ten Brink, G. Kramer, and A. Ashikhmin, "Design of low-density parity-check codes for modulation and detection," *IEEE Trans. Commun.*, vol. 52, no. 4, pp. 670–678, Apr. 2004.

[34] A. Ashikhmin, G. Kramer, and S. ten Brink, "Extrinsic information transfer functions: Model and erasure channel properties," *IEEE Trans. Inf. Theory*, vol. 50, no. 11, pp. 2657–2673, Nov. 2004.

[35] T. Huang, T. Yang, J. Yuan, and I. Land, "Design of irregular repeat-accumulate coded physical-layer network coding for Gaussian two-way relay channels," *IEEE Trans. Commun.*, vol. 61, no. 3, pp. 897–909, Mar. 2013.

[36] C. Di, D. Proietti, I. Telatar, T. Richardson, and R. Urbanke, "Finite-length analysis of low-density parity-check codes on the binary erasure channel," *IEEE Trans. Inf. Theory*, vol. 48, no. 6, pp. 1570–1579, Jun. 2002.

[37] P. Tan and J. Li, "Finite-length extrinsic information transfer (EXIT) analysis for coded and precoded ISI channels," *IEEE Trans. Magn.*, vol. 44, no. 5, pp. 648–655, May 2008.

[38] Y. Fang, G. Bi, Y. L. Guan, and F. C. M. Lau, "A survey on protograph LDPC codes and their applications," *IEEE Commun. Surveys & Tutorials*, vol. 17, no. 4, pp. 1989–2016, Fourth Quarter 2015.

[39] J. Lee and R. Blahut, "A note on the analysis of finite length turbo decoding," in *Proc. IEEE Int. Symp. Inf. Theory (ISIT)*, Jun. 2002, p. 83.

[40] Y. Chen, P. Njeim, T. Cheng, B. Belzer, and K. Sivakumar, "Iterative soft decision feedback zig-zag equalizer for 2D intersymbol interference channels," *IEEE J. Sel. Areas Commun.*, vol. 28, no. 2, pp. 167–180, Feb. 2010.

[41] M. Franceschini, G. Ferrari, and R. Raheli, "Does the performance of LDPC codes depend on the channel?" *IEEE Trans. Commun.*, vol. 54, no. 12, pp. 2129–2132, Dec. 2006.